Article citation info:
Palkus K. Numerical analysis of front deflector at outer air seal of low pressure turbine. Combustion Engines. 2026;206(3):121-129. https://doi.org/10.19206/CE-217829

Kacper PALKUS

Combustion Engines
Polish Scientific Society of Combustion Engines

Numerical analysis of the front deflector at the outer air seal of low-pressure turbine

ARTICLE INFO

Received: 15 November 2025
Revised: 28 January 2026
Accepted: 5 February 2026
Available online: 12 February 2026

A new design solution – the front deflector – intended to improve the performance of the outer air seals of the low-pressure turbine is analyzed in this paper using steady Reynolds-Averaged Navier-Stokes (RANS) simulations of a three-stage, state-of-the-art LPT model, including inner and outer cavities. The regions near the casing in the LPT still show potential for improvement, mainly due to flow interactions associated with the outer air seals. One recent concept for improving these areas is the front deflector. The solution is to modify the front part of the cavity. Its operating principle is to introduce an additional labyrinth for the leakage while simultaneously minimizing the front cavity volume. In the paper, several scenarios for implementing this feature are analyzed, including reducing the front-cavity volume without a static fin and adding a static fin to create an auxiliary labyrinth. Furthermore, the effects on the flow and the potential improvements in LPT efficiency associated with the solution are discussed. The former reduces front-cavity recirculation and its interaction with the mainstream; the latter reduces seal leakage when the fin length is sufficient. Across three stages, the predicted changes in LPT isentropic efficiency are on the order of 0.03–0.06%, depending on the scenario.

Key words: *front deflector, outer air seal, low-pressure turbine, efficiency, new design, CFD*

This is an open access article under the CC BY license (http://creativecommons.org/licenses/by/4.0/)

1. Introduction

There is considerable interest in improving the turbomachine sealing system because it directly affects the performance of the entire engine. Enhancement in performance can be achieved by either boosting or altering the thermodynamic cycle or increasing the efficiencies of particular components [4].

Efficient operation of the low-pressure turbine is of high importance at the component level. activities aimed at improving the efficiency of this module are meaningful for the environment, airlines, and engine producers.

On the other hand, modern CFD-assisted designs of turbomachinery are already considerably loaded and optimized. The application of high-tech solutions, such as low-loss airfoils via controlled laminar-turbulent boundary-layer transition, ultra-thin trailing edges, optimized work distribution, endwall contouring, and other technologies, has enabled the edges of maximal efficiency in today's low-pressure turbine (LPT).

As a result, the overall isentropic efficiency of the best designs is already very high for the currently optimized designs, and gains of the order of 0.1% in isentropic efficiency are difficult to achieve; however, they are still highly required [19].

Nonetheless, there are a few areas requiring further development. The potential still exists in regions at the sides of the main gas path [19], where inner and outer air seals can be differentiated. Sealing systems in low-pressure turbines are indispensable because they ensure proper engine operation. Nevertheless, as reported by different researchers, they inevitably decrease efficiency by as much as a few percentage points [9, 22].

In this paper, the main focus is on the outer air seals (OAS) of LPT. A representative state-of-the-art outer air seal is shown in Fig. 1. It comprises a labyrinth seal created between the blade fins and an abradable structure e.g. honeycomb. Labyrinth seals are effective and reliable. They are already very well-grounded solutions, robust and proven – perfect for aircraft engines as highlighted in [17]. This type of sealing can withstand high demands and harsh conditions in outer cavities.

As indicated by Hendricks et al. [10], sealing requirements vary significantly between shroud regions at blade tips and near the shaft for sealing of platform and cavity interfaces. IAS are located near the disk regions, OAS in the vicinity of the casing. As a result, the outer seals operate at twice the radius of the inner cavities at very high circumferential speeds. Typically, the outer air seals configurations consist of two or, at most, three fins. It is because additional mass at such a radius is unfavorable for the durability of the rotating blade. Between the two locations, there are also meaningful differences in pressure gradients, thermal and structural requirements. Another challenge posed by materials capabilities – not only due to the temperature level but also with respect to contact at the interface between rotating and nonrotating parts, as pointed out by Chupp et al. [3]. Furthermore, there are significant relative radial and axial movements of the parts. As a result, it is extremely difficult to maintain relatively small clearances between rotating and nonrotating parts in these regions. Another notable distinction between the inner and outer sealing regions is the amount of cooling flow. OAS experiences much less purging and, as a result, operates at higher temperatures, which is limiting for many solutions.

Despite the ongoing need for enhancements to the sealing system, various solutions cannot be implemented for OAS due to the range of abovementioned multidisciplinary limitations. For instance, a promising advance in sealing is brush seals, which can be configured in different ways [2, 3, 12]. The sealing performance of brush seals is superior to that of conventional labyrinth seals. At a certain clearance, they can reduce leakage by up to 80% compared to the straight labyrinth [3]. While brush seals are suitable for compressors and some turbine internal locations, they are

not applicable to OAS for several reasons, including substantial variations in clearances, reliability at high temperatures, and deterioration and oxidation of wires [3, 6].

Different researchers have applied modifications to the OAS cavities to improve inflow to the mainstream and reduce leakage. In a typical arrangement, fins point upwards from the blade shroud. Mahle and Schmierer [16] proposed applying an inverse fin configuration, typical of steam turbines, to an aircraft LPT. Klingels [14] proposes a combined configuration of conventional and inverse fin designs. Besides two conventional fins at the LPT blade shroud, in the rear part of the cavity, his design includes another static fin that points down. Features in the rear part of OAS are also researched by Rosic et al. [23]. The authors investigate three different concepts: shaping of the rear part of the exit cavity, an axial deflector, and a radial deflector in several geometrical variations. Most designs demonstrate the positive impact of the devices in the rear cavity. Nevertheless, the application of such devices to OAS of LPT is problematic due to the considerable axial rotor movement, which limits most such solutions. A recent idea by Nishii and Hamabe [18] proposes a secondary-flow suppression structure in the rear part of a cavity. It is an additional radial opening of the rear cavity. In this way, the leakage flow is expected to decrease slightly. In this configuration, the blade's movements are not restricted. Fanelli et al. [5] propose another solution, suggesting the incorporation of small airfoil-shaped structures in specific locations along the blade shroud. A good example of a well-performing advance with respect to outer seals is the application of a separate active clearance control system to the low-pressure turbine. It has become state-of-the-art for today's turbines. It provides an increase in LPT performance on the same basis as for high-pressure turbines, by maintaining radial clearances at a consistently low level throughout the mission.

Sealing systems for turbomachinery are constantly evolving, with ongoing development of available solutions and recent advances. However, due to various limitations in novel low-pressure turbines, many of these concepts are not applicable.

The objective of this paper is to analyze the front deflector (FD) as a new concept for outer air seals. The developed solution is intended to be simple and straightforward for implementation. The research primarily focuses on the aerodynamic operation and key sensitivities of the solution, providing directions for its further development. Furthermore, the research contributes to a deeper understanding of OAS operations, particularly in relation to the effects associated with the proposed designs. Front deflector concept and its initial multidisciplinary evaluation.

1.1. Baseline case – state-of-the-art LPT OAS

The solution discussed in this paper is intended for improving LPT operation in the area of outer air seals. Figure 1 presents a typical OAS design for LPT, which is chosen as the baseline. It is a labyrinth seal with two fins and an abradable honeycomb structure.

The functional principle of this sealing system is based on creating a labyrinth of fins and a honeycomb, effectively reducing the leakage mass flow rate over the blade and, consequently, overall losses and increasing machine performance. The leakage goes through the fins and further inflows into the mainstream before the subsequent vane.

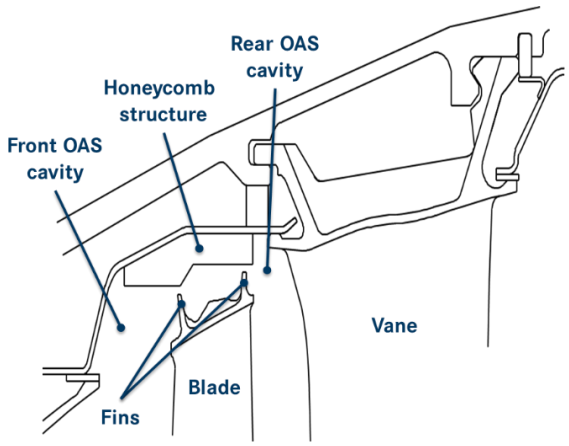

Fig. 1. Schematic representation of a state-of-the-art Outer Air Seal of LPT EP3324002B1 [14]

It is important to note that the blade moves relative to the non-rotating parts during the mission of an engine, due to thermal and structural displacements. Thus, it is not possible to design anything in the area of the blade movements. Interaction between the blade and the honeycomb is allowed. In regular operation, the fins rub into the honeycomb. In addition, it should be noted that the LPT may be equipped with the ACC system, providing tight running clearances over the mission.

The discussed design is a well-established configuration of the outer air seal, proven to be robust and reliable throughout the LPT's life cycle.

1.2. New solution - Front Deflector

The concept developed to improve the OAS is the front deflector. It is schematically pictured in Fig. 2, which follows patent application [20], confirming the novelty of the solution. It is a modification of the front part of the OAS cavity. The underlying principle of the concept is to introduce an additional labyrinth to reduce leakage and to minimize the front volume.

The labyrinth is intended to reduce leakage through the seal. By decreasing the cavity volume, the gas path contour approaches the ideal flow path, reducing interactions between the large vortices in the OAS cavity and the mainstream. It is expected that the solution will further improve performance in off-design operation when the blade moves close to the deflector. Additionally, the front fin of the blade can be inclined towards the static fin to improve the overlapping labyrinth.

The assessment indicates that it is a relatively simple solution that enhances the front part of OAS.

The length of the static fin depends on the blade's keep-out zones, which vary by machine. There are various ways to realize the front deflector concept; however, the aerodynamic benefits of the front deflector depend on the primary geometrical features that influence the cavity volume.

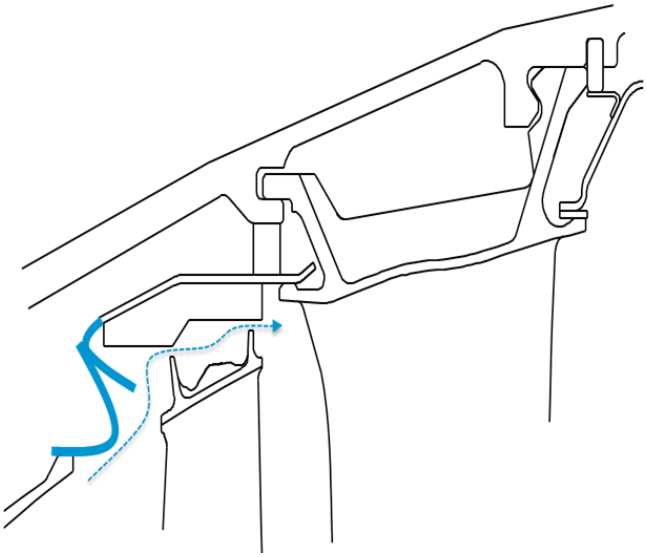

Fig. 2. Schematic representation of the front deflector concept. Reference patent EP19209602A1 [20]

The deflector is expected to provide aerodynamic advantages at the LPT design point and during off-design operation, as the blade moves closer to the deflector due to the rotor's axial movement relative to the casing. In these operating conditions, the feature will provide additional sealing improvement.

2. Numerical CFD modeling

2.1. Geometry and mesh

To evaluate the aerodynamic benefits of the Front Deflector, the feature is designed for all stages of the researched LPT. It is analyzed in several configurations, using CFD to assess the aerodynamic efficiency benefit. The CFD model of the turbine reflects an aerodynamic 3-stage rig of a modern LPT. Figure 3 provides a visual representation of the machine.

Accurately reflected geometry is of primary importance for numerical prediction. Therefore, airfoils, including all meaningful details, are thoroughly modeled. In addition, the model incorporates cavities at the inner and outer endwalls. As demonstrated by Gier et al. 0, the inclusion of cavities is of significant importance for the reliable prediction of the LPT flow field and its characteristics, particularly for efficiency. Similar conclusions were drawn by Giboni et al. [8] and Henke et al. [11].

The machine-discretization approach corresponds to the procedure used by Mahle [15]. It assumes separate meshing of the mainstream and the cavities, which enables high-quality grids. Structured, hexahedral meshes are generated for both the main gas path and the cavities. The complete mesh consists of around 24 million cells, including 6 million representing cavities. The grids are refined at walls and in regions of high gradients, e.g., at the fins of the labyrinth seals. The averaged dimensionless wall distance y+ is around 1 at the airfoils and at the endwalls in the mainstream. This contributes to the proper resolution of boundary layers. Resolution at the cavity walls is intentionally coarser. It is also considered that resolving the boundary layers in the cavities would significantly increase the model size. Thus, Wall Functions are applied in these regions. The justification of this approach for outer air seals is broadly described in [19].

The quality of the meshes is considered very good and meets best practices for the applied CFD solver. Exemplary grids for a cavity are shown in Fig. 5.

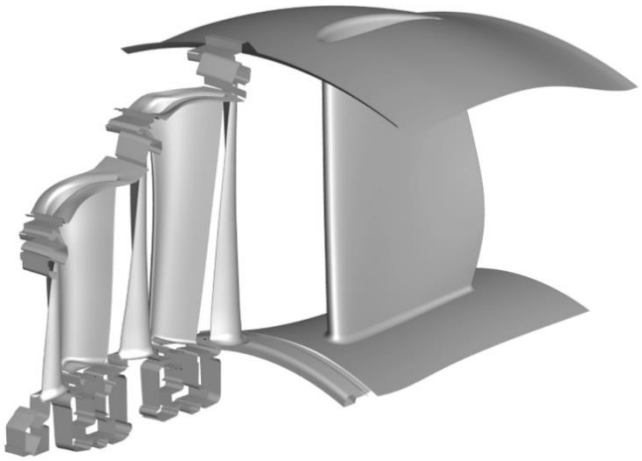

Fig. 3. CFD model of the analyzed LPT

2.2. CFD setup

For the efficiency assessment, numerical steady-state Reynolds-Averaged Navier-Stokes simulations were conducted. Wein et al. [25, 26] performed high-quality measurements of a straight outer air seal and compared them with RANS and Large Eddy Simulations. They demonstrate the potential application of properly configured RANS for OAS analyses. Their findings indicate that, despite local deviations in flow behavior, RANS delivers robust and valid predictions of the primary flow features that drive phenomena in the outer cavities. RANS also remains the industrial standard and is deemed sufficient for many turbine research as pointed by Vanhaelst et al. [24].

For the analyses, the TRACE solver, specialized for turbomachinery applications, has been employed. It is a density-based code, developed by the German Aerospace Center (DLR) and MTU Aero Engines. TRACE uses a predictor-corrector solution strategy. It allows fully implicit discretization of the equations at a given time step. Higher resolution spatial discretization schemes are used. For TRACE, it is the second-order accurate Fromm scheme [7], together with a special van Albada limiter [1] to stabilize the solving process. For time integration, implicit procedures are used until a steady state is reached.

The two-equation Wilcox k-ω model [27] is used for turbulence modeling. As verified by Gier et al. [9] and Henke et al. [11], it provides reliable prediction with respect to low-pressure turbines, including cavities, for a range of Reynolds numbers typical for aircraft engines. The setup also includes other extensions; in particular, the turbulence model is corrected by the Kato-Launder [13] formulation to account for turbulent kinetic energy production at stagnation points.

2.3. Boundary conditions

The low-pressure turbine under investigation is simulated at its design point. At the inlet of the CFD model of the turbine, boundary conditions measured in the test rig are specified. This includes radial distributions of total pressure, total temperature, turbulence quantities, and velocity angles. At the outlet, static pressure is set, assuming radial equilibrium. Both the inlet and the outlet are non-reflecting. The boundary conditions imposed at the walls are shown in Fig. 4. All walls are assumed to be adiabatic.

In steady simulations, the rows in the mainstream are connected via mixing planes, following the typical approach used in turbomachinery simulations. This way enables the connection of vanes and blades with different speeds and pitches defined in the flow domains.

Also, in the cavities and at necessary locations, mixing planes between stationary and rotating domains are specified. Additionally, special interfaces, described by Yang [28], are used to connect the cavities and the mainstream. The approach is illustrated in Fig. 4. The interfaces facilitate the transfer of numerical information between the two sides, modeling inflow or outflow. To ensure proper connection between the two, the grids at the interfaces are adjusted to provide a similar resolution on both sides.

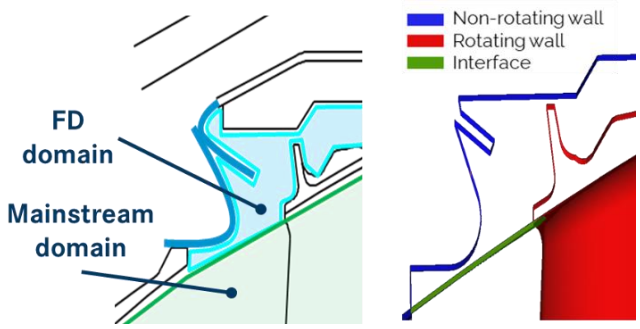

Fig. 4. CFD modeling of the front deflector

2.4. Convergence behavior

The simulations are considered converged after revising several conditions. Parameters of the machine, such as mass flow, pressure ratio, and efficiency, are monitored for the entire system and for individual rows at specified intervals. Additionally, the behavior of averaged flow quantities at interfaces is monitored to ensure solution stability. The global and maximal residuals are also monitored. For all simulations in this article, the global RMS residuals are fairly below $1 \cdot 10^{-5}$. The simulations are stopped manually once a prolonged steady state is reached, provided that the above criteria are met. For all researched cases, the efficiency fluctuations were an order of magnitude smaller than reported changes.

2.5. Introduction of the front deflector to the baseline CFD model

As previously mentioned, the modification reflecting the front deflector is applied to the outer air seals for all stages of the reference LPT. Figure 5 indicates the crucial geometrical parameters of the front deflector. Those are the protrusions of the deflector covering the front cavity volume and the length of the static fin. In the researched configurations at different stages those parameters vary $a_x = 0.4 - 0.5\ b_x$ and $L = 0.7 - 1.2\ H$.

The modeling approach is depicted in Fig. 4. The fluid control domain of the cavity, including the surrounding area of the feature, is modeled and appended to the main gas path with interfaces. The setup applied to the modified cases corresponds to that used in the reference turbine.

Figure 5 also presents meshes for different configurations of the front deflector. The cases represent: baseline outer air seal; cavity with reduced front volume without a static fin; and front deflector with a static fin.

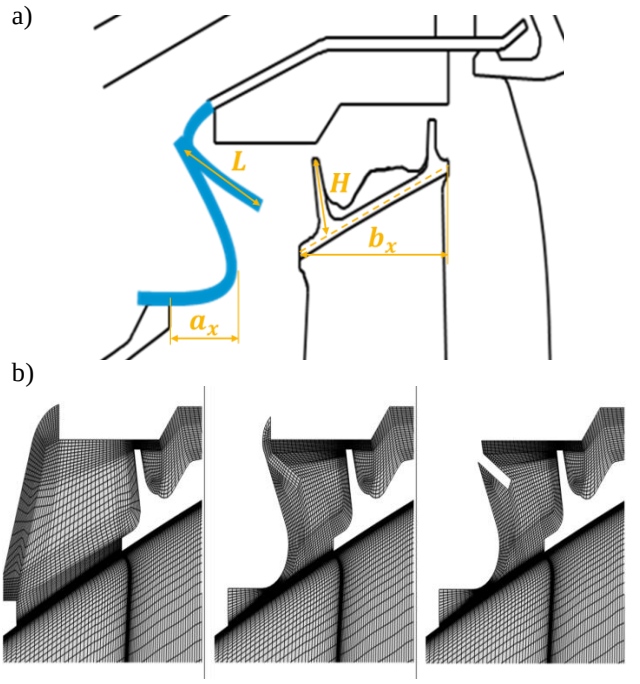

Fig. 5. Primary geometrical parameters of front deflector (a), comparison of the meshes for different configurations. From the left: reference cavity, front deflector without static fin and front deflector with static fin

The changes to the mesh are kept to a minimum level – only the front part of the cavity is modified. In particular, the number of cells at the interface is the same for all configurations. The region near the fin of the blade is already unchanged. A small refinement is necessary in the vicinity of the additional static fin, which is deemed acceptable. Mesh criteria for the modifications are also considered acceptable.

The validity of the applied CFD models is comprehensively discussed in [19]. The findings confirm high accuracy of the prediction for the outer air seals using the employed numerical method. It is concluded that modifications to the OAS, which affect the mainstream flow, can be quantified in terms of changes in turbine efficiency. The overall LPT isentropic efficiency is calculated between LPT inlet and outlet as:

$$\eta_{LPT} = \frac{h_{t,out} - h_{t,in}}{h_{t,out,is} - h_{t,in}} \quad (1)$$

3. Results and discussion

3.1. Evaluation of the performance of the front deflector without the static fin

At first, the aerodynamic performance and benefits resulting from reducing the front OAS cavity with the front deflector without a static fin are assessed. Two configurations, as shown in Fig. 6, are analyzed and compared to the baseline case.

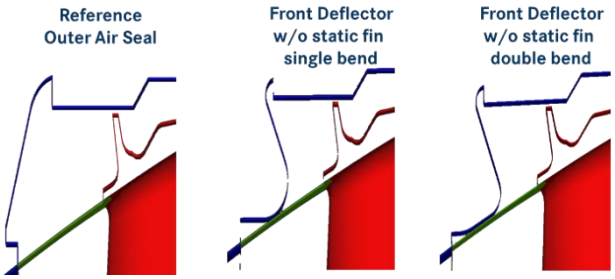

Fig. 6. Investigated cases of front cavity reduction with front deflector without static fin

The first modification represents the feature geometry with a single bend, while the second uses a double bend. The solution with two bends allows for reducing the step and achieving a very close reproduction of the ideal flow path. In this way, it is assumed that step losses can be further reduced. According to Gier et al. [9], the significance of step losses increases for smaller leakages through the seal, which is often the case in today's turbines due to advanced systems for running clearance reduction. Thus, looking for fractions of efficiency, it is also worth checking this direction for improvements.

Detailed CFD simulations of all cases, presented in Fig. 7, indicate that both solutions are beneficial but perform nearly equally.

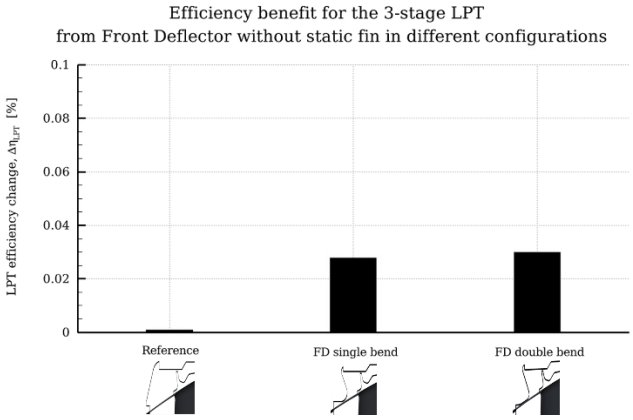

Fig. 7. LPT efficiency benefits from front cavity reduction with front deflector without the static fin

The overall benefit is considered comparable between the two configurations. This indicates that such a small additional step in the flow path, which adds an additional perturbation to the fluid, has a relatively small impact on the overall improvement. Figures 8 and 9 present the flow field of the investigated cases.

As evident from these figures, the large vortices in the front cavity are considerably reduced when the cavity volume is decreased. The primary benefit is indeed the reduction in interactions.

As shown in Fig. 8, the front cavity recirculation zones interact with the mainstream, generating shear losses due to the difference in circumferential velocity between the two flows.

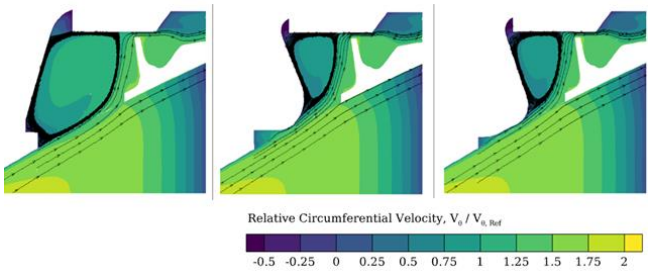

Fig. 8. Relative circumferential velocity and streamlines for investigated cases of front deflector without static fin in different configurations

Moreover, the figure reveals that, in addition to contributing to the reduction of the vortex, the FD simultaneously reduces the circumferential velocity in the front part of the cavity, which is closer to the mainstream velocity. Consequently, the mixing losses are smaller, as also indicated by Fig. 9.

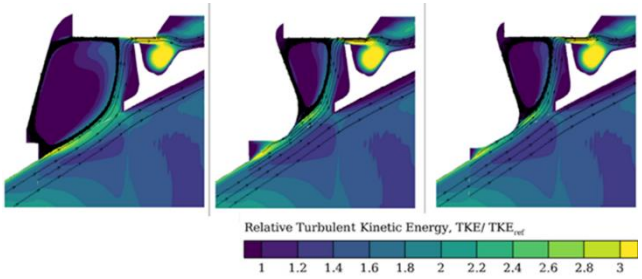

Fig. 9. Relative turbulent kinetic energy and streamlines for investigated cases of front deflector without static fin in different configurations

Table 1. Comparison of the characteristic numbers for OAS with front deflector without static fin for different configurations for one stage

	Reference	FD single bend	FD double bend
			
Axial Reynolds number, Re_{ax}	1760	1760	1760
Outlet Swirl ratio, K_{out}	0.68	0.66	0.66
Windage heating, σ	0.19	0.19	0.19

As shown in Fig. 8 and Fig. 9, the primary leakage path is not affected by the presence of the front deflector without the static fin. This observation is further supported by the dimensionless numbers for OAS [21], provided for one seal across different FD variants in Table 1. These quantities

are: axial Reynolds number, swirl ratio and windage heating according to the equations below:

$$\mathrm{Re}_{ax} = \frac{\dot{m}}{2\pi R\mu} \tag{2}$$

$$K = \frac{V_\theta}{NR} \tag{3}$$

$$\sigma = \frac{2c_p(T_{t,out} - T_{t,in})}{U^2} \tag{4}$$

For all variants, the characteristic numbers are nearly the same. It indicates that the seal's general operation remains unchanged across the investigated designs of the concept without a static fin. In particular, the axial Reynolds number [21], which provides insights into leakage behavior, is comparable. Thus, it is concluded that reducing the front cavity volume does not affect leakage through the seal, suggesting it is not the reason for the observed benefit in the cases without the static fin.

Reducing the front cavity volume with the front deflector (without the static fin) consistently weakens the large vortices in the front cavity and lowers their interaction with the mainstream, leading to a small but repeatable LPT efficiency benefit around 0.03% for the solution implemented in all stages. Leakage behavior remains unchanged, indicating that the improvement results solely from reduced cavity–mainstream interaction rather than from any modification of the seal leakage.

3.2. Evaluation of the performance of the front deflector with the static fin

The static fin creates an additional labyrinth for leakage and, in this way, reduces it. To assess the sensitivity of the FD concept to the length of the fin, two cases are considered: a short fin and a long fin. These variants are compared with the reference OAS design and with the case without a static fin. The investigated configurations are presented in Fig. 10.

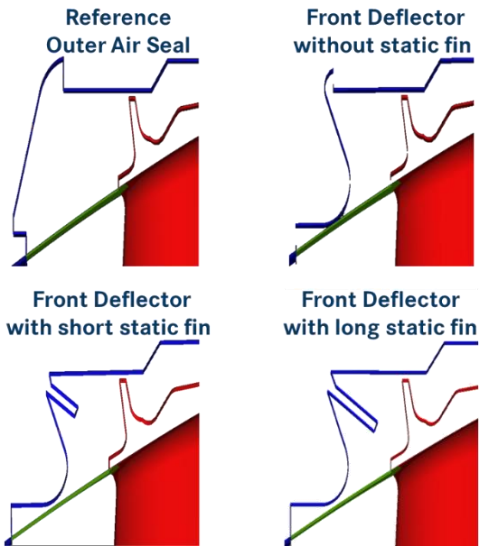

Fig. 10. Investigated design cases of the front deflector with a static fin

Analyzing the flow field shown in Fig. 11, it is apparent that the vortex present in the front cavity is further reduced with the application of the static fin. Nevertheless, revising the benefit in LPT efficiency presented in Fig. 13, it is evident that the short static fin does not provide any further improvement compared to the front deflector without the static fin. It can be concluded that a decrease in the vortices in the front cavity has a meaningful impact only if it reduces their interaction with the mainstream.

This is reflected in Fig. 11, which compares the two cases by the relative TKE level and the lack of influence on the streamlines due to the leakage. Thus, the short fin does not function as intended, as its primary purpose is to create an additional labyrinth to reduce leakage. It is additionally confirmed in Table 2 by comparing the axial Reynolds number [21].

It points to a conclusion that the length of the fin is crucial for the overall benefit from the solution. It is evident that as the clearance between the blade and the static fin decreases, the leakage encounters more blockage, resulting in its reduction. Nevertheless, it is important to ensure the blade does not come into contact with the fin to avoid damage. Taking this into account, further investigation of the case with the longer fin is conducted.

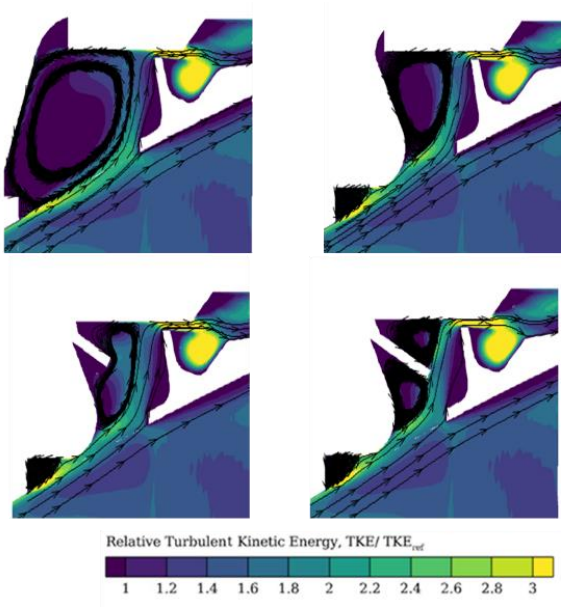

Fig. 11. Relative turbulent kinetic energy and streamlines for investigated cases of front deflector with static fin in different configurations

As noticeable in Table 2, the analyses show that the front deflector with the longer static fin reduces the axial Reynolds number [21] of the investigated OAS. The figure shows that the longer fin reduces leakage by around 6% compared to the reference case. This reflects positively on the efficiency gain, as depicted in Fig. 13.

Moreover, Table 2 shows that applying the front deflector does not visibly affect the outlet swirl ratio or windage heating [21]. Only in the configuration with the long static fin is a small change in the outlet swirl observed. Thus, it is concluded that in the rear part of the cavity and behind it, the mixing as well as internal losses are not noticeably changed with the application of the front deflector. This is also confirmed by revising plots in Fig. 11, because already

in the vicinity of the first fin, there are no significant differences between the configurations.

Table 2. Comparison of characteristic numbers for OAS with a front deflector and with static fin for different configurations

	Reference	FD without static fin	FD with short static fin	FD with long static fin
				
Axial Reynolds number, Re_{ax}	1760	1760	1750	1650
Outlet swirl ratio, K_{out}	0.68	0.66	0.65	0.64
Windage heating, σ	0.19	0.19	0.19	0.19

Further insight into the flow above the first fin is shown in Fig. 12 below. It provides profiles of relative velocity above the first fin of the seal. This comparison clearly shows that the front deflector concept has no significant influence on the velocity. Upon analysis, only a small decrease of up to 6% can be observed. This decrease is visible for both axial and circumferential components.

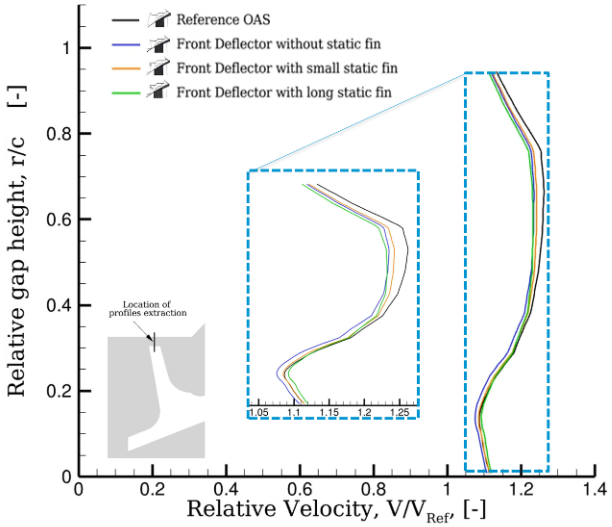

Fig. 12. Profile of relative velocity above the first fin of the outer air seal for different configurations of the front deflector

Based on Fig. 13, the overall efficiency potential of the front deflector concept is estimated to lie between 0.03% and 0.06%, depending on the length of the static fin. As pointed out earlier, the configuration with the short static fin is close to the variant without a static fin. Thus, for turbines where the length of the fin is significantly limited due to keep-out zones of the blade, it is applicable to omit the static fin. Additionally, it is anticipated that the concept can yield further benefits when combined with inclined fins to enhance the efficiency gains.

The addition of a static fin improves performance only when the fin is long enough to act as an effective additional labyrinth. While the short fin does not reduce leakage, the long fin reduces OAS leakage and yields a higher LPT efficiency gain of up to 0.06% for the solution implemented across all stages. Other flow characteristics remain largely unchanged, highlighting fin length as the key parameter influencing the benefit.

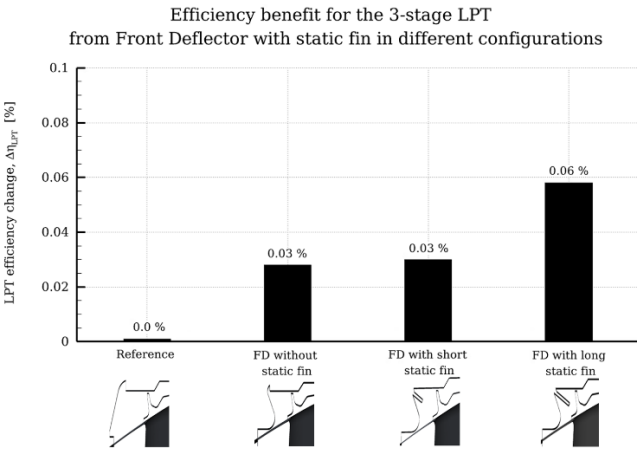

Fig. 13. LPT efficiency benefit from front deflector in different configurations

4. Future work

Analyses of cases with the longer fin indicate the feature could have potential in off-design operation when the blade moves forward. Verifying this requires future work.

Furthermore, successful implementation in an engine requires a detailed assessment of durability, mechanical robustness, and manufacturability of the proposed geometry.

Experimental validation of the specific designs also remains outstanding and is essential to confirm the numerical findings presented herein.

5. Conclusions

This work investigated a new front deflector concept for outer air seals in a low-pressure turbine, aiming to improve near-casing aerodynamic performance at minimal integration cost, while simultaneously providing a small overall efficiency benefit.

The assessment was carried out on a three-stage, state-of-the-art LPT configuration with detailed inner and outer cavities using steady RANS simulations.

The concept has been investigated in two main configurations – with and without the static fin. The feature improves OAS performance in two ways. Firstly, it reduces interactions between the mainstream and the front cavities for all investigated configurations.

Secondly, it provides an additional labyrinth for the leakage reduction in the configuration with the long static fin.

The efficiency gain in the case without the static fin results from reduced interactions in the front cavity. The reduction in the front cavity volume does not influence the leakage through the seal, yielding a small but repeatable efficiency benefit.

It is observed that the inclusion of a static fin reduces leakage only if it is long enough, and this depends strongly on the turbine's design.

The overall improvement in LPT efficiency from the front deflector implemented across all three stages is between 0.03% and 0.06%, depending on the application. The

final benefit must be weighed against implementation costs to justify its adoption in engines.

Acknowledgements

The author would like to express sincere gratitude to MTU Aero Engines for the permission to publish the research.

Nomenclature

a_x	[m]	axial protruding of FD
b_x	[m]	axial shroud length
c	[m]	radial clearance
c_p	[J/(kg·K)]	specific heat capacity
h	[J/kg]	specific enthalpy
H	[m]	first fin height
L	[m]	FD static fin length
$\dot{m}$	[kg/s]	mass flow rate
K	[–]	swirl ratio
N	[rpm]	rotational speed
R	[m]	average radius of fins
Re_{ax}	[–]	axial Reynolds number
Ref		any reference quantity
T	[K]	temperature
$U = \frac{\pi N}{30} R$	[m/s]	rotor fins circumferential velocity
V_x	[m/s]	axial velocity component
V_r	[m/s]	radial velocity component
V_θ	[m/s]	circumferential velocity component
η	[–]	isentropic efficiency
μ	[Pa·s]	dynamic viscosity
σ	[–]	windage heating
Δ		change in any quantity
FD		front deflector
IAS/OAS		inner / outer air seal
LPT		low pressure turbine
TKE		turbulent kinetic energy

Bibliography

[1] Albada van GD, Leer van B, Roberts W. A comparative study of computational methods in cosmic gas dynamics. Astron Astrophys. 1982;108(1):76-84. https://ui.adsabs.harvard.edu/abs/1982A%26A...108...76V/abstract

[2] Brush seals: World-class sealing technology. MTU Aero Engines. 2014. Report No. EN10/20/MUC/00500/AD/RI/D.

[3] Chupp RE, Hendricks RC, Lattime SB, Steinetz BM. Sealing in turbomachinery. NASA, Glenn Research Center, Cleveland, USA, NASA Technical Memo. NASA/TM-2006-214341. 2006.

[4] Dewanji D, Rao AG, van Buijtenen JP. Conceptual study of future aero-engine concepts. Int J Turbo Jet Engines. 2010;26(4):263-276. https://doi.org/10.1515/TJJ.2009.26.4.263

[5] Fanelli JJA, Bassery JJA, Dupeyre RJP, Francois EL. Aube mobile pour une roue d'une turbomachine. Applicant: Safran Aircraft Engines. Patent No. FR3092864A1. 2020.

[6] Flitney RK. Seals and sealing handbook. Ed 6th. Butterworth-Heinemann. 2007. https://doi.org/10.1016/B978-0-08-099416-1.00002-4

[7] Franke M, Kugeler E, Nurnberger D. Das DLR-Verfahren TRACE: Moderne Simulationstechniken für Turbomaschinenströmungen. In: DGLR-Jahrbuch. Deutscher Luft- und Raumfahrtkongre; 2005 Sep 26-29.

[8] Giboni A, Wolter K, Menter JR, Pfost H. Experimental and numerical investigation into the unsteady interaction of labyrinth seal leakage flow and main flow in a 1.5-stage axial turbine. Proceedings of ASME Turbo Expo 2004; 2004 Jun 14–17; Vienna. https://doi.org/10.1115/GT2004-53024

[9] Gier J, Stubert B, Brouillet B, de Vito L. Interaction of shroud leakage flow and main flow in a three-stage LPT. J Turbomach. 2005;127(4):649-658. https://doi.org/10.1115/1.2006667

[10] Hendricks RC, Chupp RE, Lattime SB, Steinetz BM. Turbomachine interface sealing. NASA Technical Memorandum NASA/TM – 2005-213633. 2005.

[11] Henke M, Wein L, Kluge T, Guendogdu Y, Biester MH, Seume JR. Experimental and numerical verification of the core-flow in a new low-pressure turbine. Proceedings of ASME Turbo Expo 2016; 2016 Jun 13-17; Seoul. ASME. https://doi.org/10.1115/GT2016-57101

[12] Justak JF. Hydrodynamic brush seal. Patent US6428009B2. 2001.

[13] Kato M, Launder BE. The modeling of turbulent flow around stationary and vibrating square cylinders. 9th Symposium on Turbulent Shear Flows. Kyoto 1993. https://api.semanticscholar.org/CorpusID:117728958

[14] Klingels H. Sealing system for a turbomachine and axial flow turbomachine. Patent EP3324002B1. 2021.

[15] Mahle I. Improving the interaction between leakage flows and main flow in a low pressure turbine. ASME. 2010;GT2010-22448:1177-1186. https://doi.org/10.1115/GT2010-22448

[16] Mahle I, Schmierer R. Inverse fin arrangement in a low pressure turbine to improve the interaction between shroud leakage flows and main flow. ASME. 2010;GT2010-22448:1177-1186. https://doi.org/10.1115/GT2011-45250

[17] NASA Conference, Seal/Secondary Air System Workshop. NASA/CP-2009-215677. 2008:131-193.

[18] Nishii D, Hamabe M. Secondary flow suppression structure. Patent WO2021199718A1. 2004.

[19] Pałkus K. Low pressure turbine efficiency increase by developing new concept of outer air seal. Doctoral Thesis 2024.
[20] Pałkus K, Lauer C, Schmierer R. Axial turbomachine sealing system. Patent EP3822461A1. 2021.
[21] Pałkus K, Strzelczyk PM. Dimensionless numbers relationships for outer air seal of low pressure turbine. Int J Turbomach Propuls Power. 2021;6(3):33. https://doi.org/10.3390/ijtpp6030033
[22] Pfau A, Schlienger J, Rusch D, Kalfas AI, Abhari RS. Unsteady flow interactions within the inlet cavity of a turbine rotor tip labyrinth seal. J Turbomach. 2005; 127(4):679-688. https://doi.org/10.1115/1.2008973
[23] Rosic B, Denton JD, Curtis EM, Peterson AT. The influence of shroud and cavity geometry on turbine performance: an experimental and computational study – part I and II. J Turbomach. 2008;130(4): 041002. https://doi.org/10.1115/1.2777202
[24] Vanhaelst R, Bannack C, Klose M. Comparison of two measurement methods for the determination of extended turbine maps at the eATL test bench of the Ostfalia UAS. Combustion Engines. 2017;169(2): 43-48. https://doi.org/10.19206/CE-2017-208
[25] Wein L. Large-Eddy-Simulation von Deckband labyrinthdichtungen [dissertation]. Hannover: Leibniz University Hannover 2020. https://doi.org/ 10.15488/10202
[26] Wein L, Kluge T, Seume JR, Hain R, Fuchs T, Kahler C et al. Validation of RANS turbulence models for labyrinth seal flows by means of particle image velocimetry. Proceedings of ASME Turbo Expo 2020; 2020 Sep 21–25. https://doi.org/10.1115/GT2020-14885
[27] Wilcox DC. Turbulence modeling for CFD. 2nd ed. DCW Industries 1998.
[28] Yang H, Nuernberger D, Kersken H. Toward excellence in turbomachinery computational fluid dynamics: a hybrid structured-unstructured Reynolds-Averaged Navier–Stokes solver. J Turbomach. 2006;128(2): 390-402. https://doi.org/10.1115/1.2162182

Kacper Palkus, DEng. – Faculty of Mechanical Engineering and Aeronautics, Rzeszow University of Technology, Poland.
MTU Aero Engines Polska, Jasionka, Poland.
e-mail: *kacp.palkus@gmail.com*